A Polarimetry Module for CSO/SHARC-II

G. Novak[a], D. T. Chuss[b], J. A. Davidson[c], J. L. Dotson[c], C. D. Dowell[d], R. H. Hildebrand[e]
M. Houde[f], L. Kirby[e], M. Krejny[a], A. Lazarian[g], H. Li[a], S. H. Moseley[b], J. E. Vaillancourt[e]
and F. Yusef-Zadeh[a]

[a]Northwestern University, Dept. of Physics and Astronomy, Evanston, IL, 60208, USA
[b]NASA/Goddard Space Flight Center, Greenbelt, MD, 20771, USA
[c]NASA/Ames Research Center, Moffett Field, CA, 94035, USA
[d]Caltech/JPL, Pasadena, CA, 91109, USA
[e]University of Chicago, Department of Physics and Enrico Fermi Institute, Chicago, IL, 60637, USA
[f]University of Western Ontario, Dept. of Physics and Astronomy, London, ON, N6A 3K7, Canada
[g]University of Wisconsin, Department of Astronomy, Madison, WI, 53706, USA

ABSTRACT

The Submillimeter High Angular Resolution Camera II (SHARC-II) is a 32 x 12 pixel submillimeter camera that is used with the ten-meter diameter Caltech Submillimeter Observatory (CSO) on Mauna Kea. SHARC-II can be operated at either 350 or 450 microns. We are developing an optics module that we will install at a position between the SHARC-II camera and the focus of the CSO's secondary mirror. With our module installed, SHARC-II will be converted into a sensitive imaging polarimeter. The basic idea is that the module will split the incident beam coming from the secondary into two orthogonally polarized beams which are then re-imaged onto opposite ends of the "long and skinny" SHARC-II bolometer array. When this removable polarimetry module is in use, SHARC-II becomes a dual-polarization 12 x 12 pixel polarimeter. (The central 12 x 8 pixels of the SHARC-II array will remain unused.) Sky noise is a significant source of error for submillimeter continuum observations. Because our polarimetry module will allow simultaneous observation of two orthogonal polarization components, we will be able to eliminate or greatly reduce this source of error. Our optical design will include a rotating half-wave plate as well as a cold load to terminate the unused polarization components.

1. INTRODUCTION

1.1 Submillimeter Polarimetry

The first detection of submillimeter polarization in an astronomical source was made twenty years ago[1], and since that time many investigators, working at many different telescopes, have made important contributions to the development of instrumentation, observational techniques and strategies, and theoretical models for interpreting polarization data. Several recent papers have reviewed this work.[2,3,4] Submillimeter polarimetry is important because it provides one of the best methods for observing interstellar magnetic fields in star forming regions[5] and other interstellar clouds. The idea is that magnetically aligned interstellar dust grains emit polarized thermal emission, and thus the measured direction of polarization gives the orientation of the interstellar magnetic field, as projected onto the plane of the sky.[6] The peak of the thermal emission spectrum of a typical molecular cloud falls in the submillimeter band, but it is also possible to measure polarized thermal emission from aligned grains at mid-IR[7], far-IR[8], and millimeter wavelengths. For this last wavelength range, pioneering work has been done using interferometers[9,10]. Besides the study of polarized emission from aligned grains, there are other applications of submillimeter polarimetry, such as the study of synchrotron emission from the Sagittarius A* black hole at the Galactic center, to give just one important example.[11]

Millimeter and Submillimeter Detectors for Astronomy II, edited by
Jonas Zmuidzinas, Wayne S. Holland, Stafford Withington, Proceedings of
SPIE Vol. 5498 (SPIE, Bellingham, WA, 2004) · 0277-786X/04/$15 · doi: 10.1117/12.553076

Both of the large submillimeter dishes on Mauna Kea (the James Clerk Maxwell Telescope, or JCMT, and the Caltech Submillimeter Observatory, or CSO), are making important contributions to submillimeter polarimetry.[2,12,13] The submillimeter polarimeter used at the CSO is called Hertz. It was built at the University of Chicago, and we have operated it at the CSO since 1994. Hertz is an array polarimeter that observes 32 sky positions simultaneously, and its passband is matched to the 350 micron spectral window. We next give a very brief overview of its principles of operation.[12,14,15] After entering the Hertz cryostat, the incident 350 micron radiation passes through a half-wave plate, and is then divided into two orthogonal polarization components by a series of free-standing wire grids. Each component is directed towards its own 32-pixel Helium-3 cooled bolometer array. Thus, two components of polarization are observed simultaneously. A polarimetric observation consists of a series of short photometric observations made at different half-wave plate angles. Each photometric observation involves chopping and nodding, as described in section 1.3 below.

1.2 A polarimetry module for SHARC-II

The CSO has recently completed the construction of a new camera, called SHARC-II (standing for Submillimeter High Angular Resolution Camera - 2nd generation) that includes a 384-pixel bolometer array and has very high optical efficiency.[16] We are building a polarimetry module for SHARC-II that will convert it into a polarimeter, replacing Hertz. The result will be an improvement in angular resolution (from 20 to 9 arcsec) an improvement in point source sensitivity (by about a factor of three) and a fourfold increase in the number of pixels. The increase in sensitivity is partly the result of the better optical efficiency of SHARC-II in comparson with Hertz, which is due to improvements in bolometer technology.

We expect to begin observations in early 2005. For the first year of operation, our observational goals are the following:

(1) Tracing magnetic field geometry in Bok globules and other sites of low mass star formation with sufficient sensitivity and angular resolution to isolate pseudo-disks and possibly resolve pinched magnetic fields.

(2) Polarimetry of T Tauri stars, where comparison with polarimetry at longer wavelengths will provide a new way to test for grain growth in proto-planetary disks.

(3) Polarimetry of Sgr A* at shorter submillimeter wavelengths than are otherwise accessible. This will test models for accretion by supermassive black holes.

(4) Comparisons of polarimetric maps having thousands of polarization vectors per cloud with theoretical simulations informed by the latest progress in the theory of magnetic grain alignment.

(5) Comparing degrees of polarization between the 350 and 450 micron emission from molecular clouds so as to verify the dip in the polarization spectrum near 350 microns and better locate the minimum.

1.3 Sky noise

For submillimeter observations from within the Earth's atmosphere, it is necessary to remove unwanted atmospheric background contributions to the signal. The atmosphere manifests itself in two ways. One way is through changes in atmospheric transmission, which affect the intensity of the detected astronomical signal, and the other is through variations in atmospheric emission. Removal of the background invariably involves subtracting signals from locations neighboring the source position (both in space and time). The two different types of signals measured in the observation process are usually ascribed the terms “source signal” and “reference signal”, respectively. The problem of precise background removal with the reference signals is rendered all the more important in polarimetry because of the lower levels, in relation to the background, of the signals ones tries to detect.

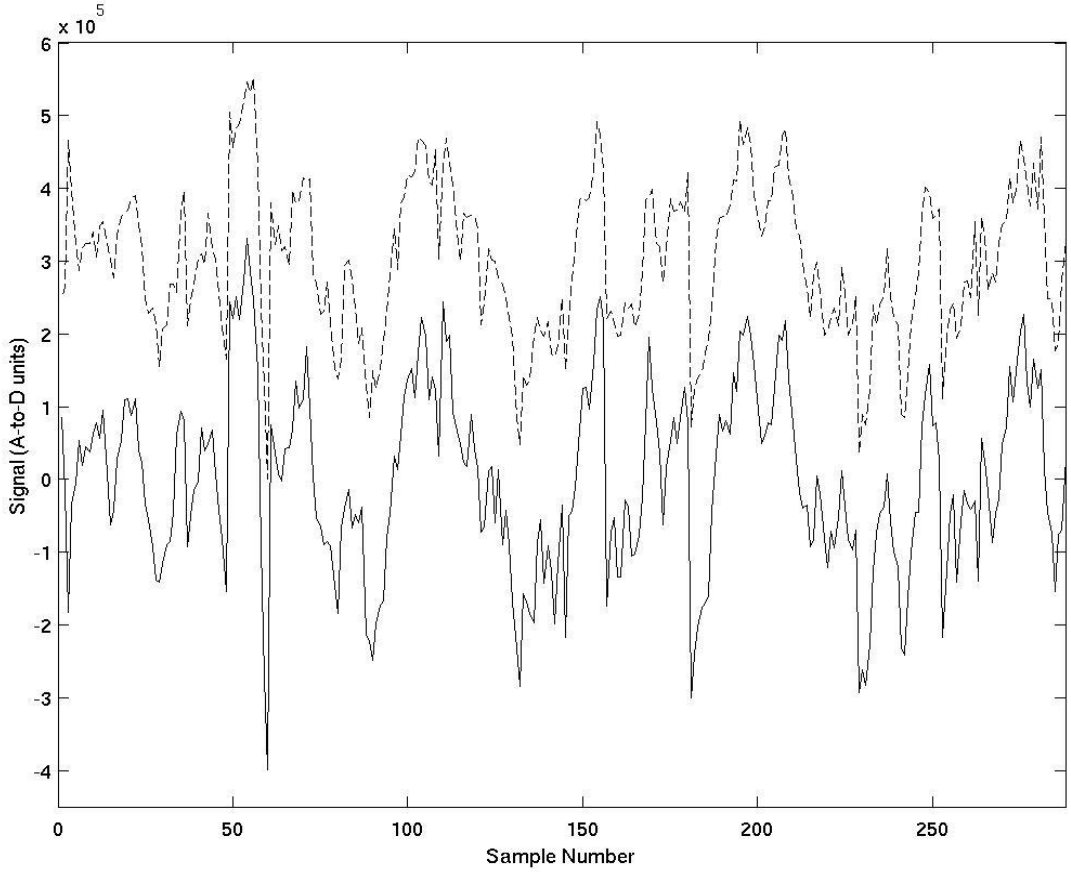

Fig. 1 - Correlated sky noise at South Pole. This figure shows the result of an eight minute integration obtained during Austral Winter 2003 with the SPARO experiment at South Pole.[17,18] The solid and dashed curves show the demodulated signals measured with two bolometers observing the same part of the sky in orthogonal linear polarizations. The dashed curve has been shifted upward for clarity. Twelve telescope nods and six half-wave plate moves were carried out during this ten minute integration, but the signals measured during telescope and half-wave plate moves are not stored by the data acquisition computer so they are not shown. The signal from the astrophysical source, G333.6–0.2, was removed to better show the sky noise.

The need for measuring signals at different locations on the sky at a fast enough rate to remove the noise from the atmosphere (and the detectors) necessitates the chopping of a mirror (usually the secondary mirror) at a sufficiently high frequency (a few Hz, typically). A slow nodding of the telescope is usually superposed to this chopping to alternatively access the reference signals symmetrically located on either side of the source.[15]

Unfortunately, even though the implementation of a chopping/nodding procedure goes a long way in reducing the adverse effects of the atmosphere, there still remain unwanted contributions in the form of "sky noise" (Fig. 1). There exist, for polarimeters that observe only one polarization component at a time, some techniques to alleviate the problem of sky noise[15], but an optimum solution takes advantage of the fact that the fluctuations in atmospheric emission and transmission (responsible for the sky noise component) are correlated for orthogonal polarization states. The SHARC-II

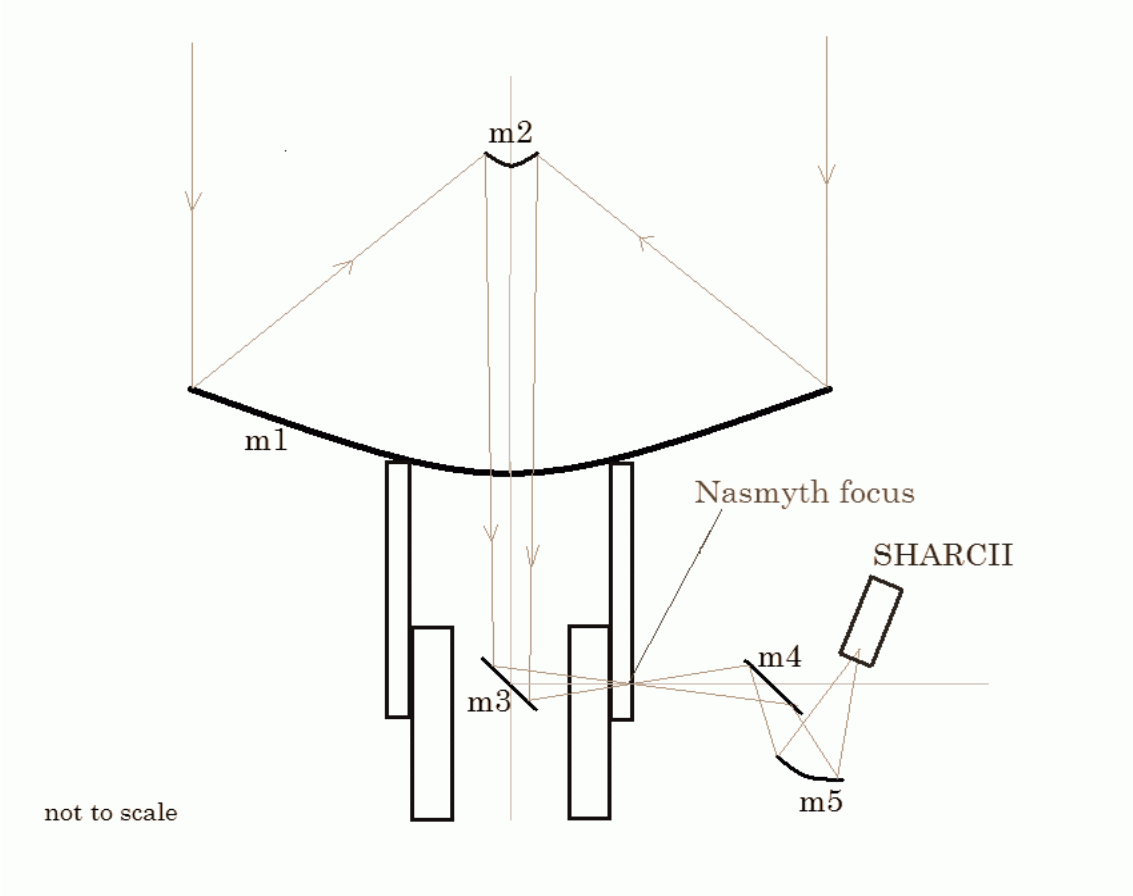

Fig. 2 - Schematic illustration of SHARC-II installed at the CSO in its planned Nasmyth location. The drawing is not to scale. The primary, m1, and secondary, m2, are shown with the telescope pointed at zenith. The rectangles beneath m1 represent the telescope support structure. The horizontal line that extends from m3 to the right coincides with the telescope's elevation axis. (SHARC-II is shown tilted but really it will be upright during its initial operation at the Nasmyth location.)

polarimeter will take full advantage of this correlation by using an optical design (see sections 1.4 and 2) that allows for efficient sky noise removal by simultaneously measuring two orthogonal polarization components. Denoting by R and T the two signals (of orthogonal polarization states) defined above, the polarization level can be measured by taking the ratio of their difference and sum

$$P = (R - T) / (R + T)$$

From this equation one can see that P is unaffected by changes in atmospheric transmission, and that fluctuations in emission are removed from the numerator. Although variations in emission are still included in the denominator, they are often small compared to the total signal intensity ($R + T$). (When they are not, the effects of sky noise can cause large errors in P, but these can be avoided by using special techniques described in section 3 below.) The preceding equation must be applied for each half-wave plate position, the resulting values of P must be combined in an appropriate way, and the instrumental polarization must be removed[15], but nevertheless this simple equation does include the advantages of doing polarimetry with dual-polarization capability.

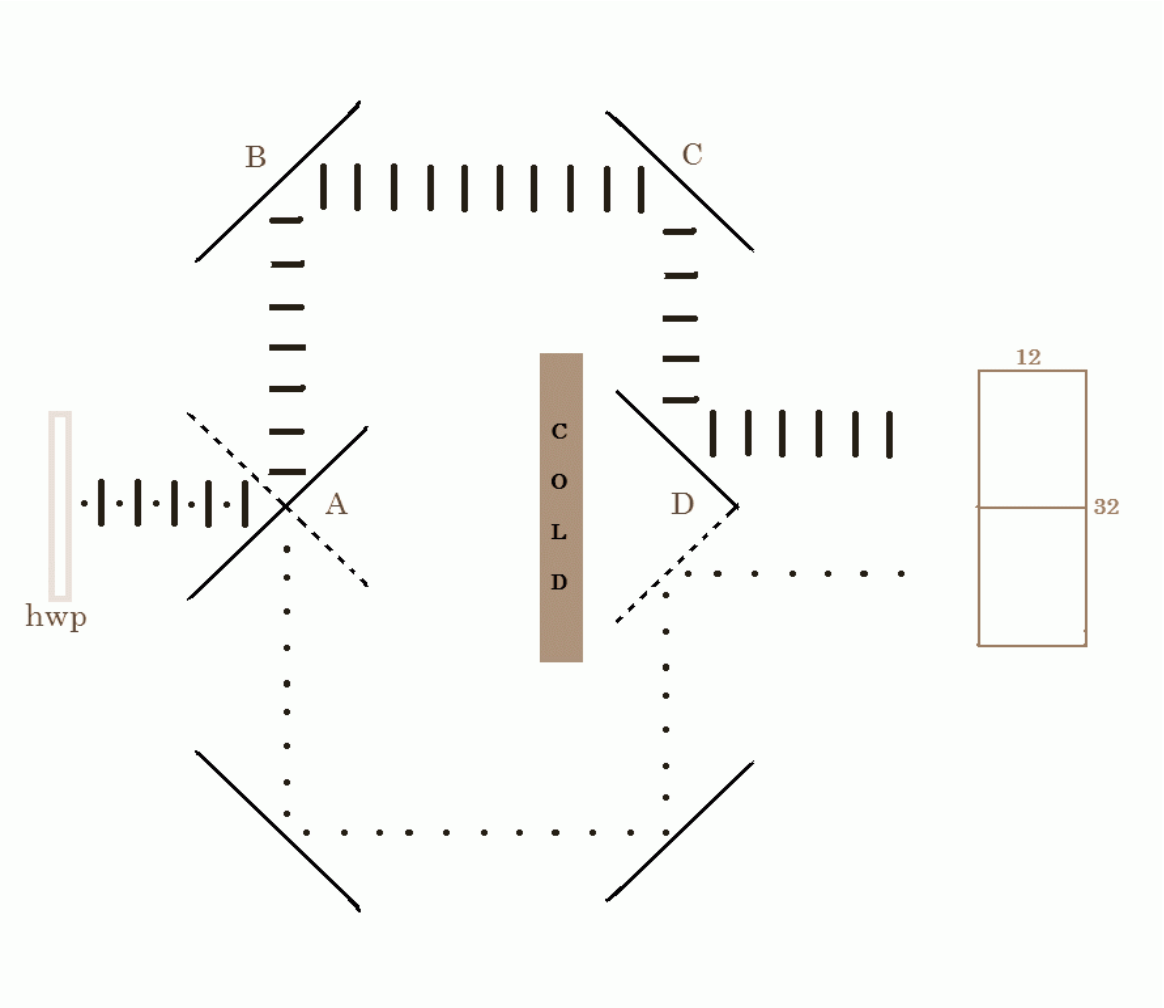

Fig. 3 - A simplified version showing the basic idea behind our polarimetry module. If it were possible to install this simple polarization module at the Nasmyth focus of the CSO, this would convert SHARC-II into a dual-beam polarimeter. In this design, the light from the primary and secondary first passes through a half-wave plate ("hwp") and is next incident upon a pair of "crossed-grids" (A). One of these grids (shown with a dashed line) has its wires oriented perpendicular to the plane of the page, while the other (solid line) has its wires running parallel to the plane of the page. B and C are mirrors, and D is another pair of grids that we refer to as the "combiner". A cold load ("COLD") is used to terminate the unused polarization components. The 32 x 12 pixel bolometer array (SHARC-II) is shown at right. The polarimetry module that we plan to build (Figure 5) is more complex, but is based on this simple idea.

1.4 Basic concept

Before describing our polarimetry module, we review the optical interface between the CSO telescope and the SHARC-II camera. SHARC-II does not sit directly at the Cassegrain focus (~ f/12) of the CSO telescope. Instead, this focus is re-imaged along a folded optical path ~2.5 m in length that includes several flat mirrors and an ellipsoidal mirror (the "relay optics"). The SHARC-II bolometer array is located at the re-imaged focal plane, which is faster (~f/4). An image of the primary (a "pupil") is located several inches in front of this focus, and SHARC-II has a cold stop at this pupil. SHARC-II and its relay optics are mounted on the alidade platform that is located behind the primary mirror.

In late Summer 2004, SHARC-II will be moved to the Nasmyth focus, as shown schematically in Fig. 2. The elevation axis of the CSO is located roughly 2 m behind the hole in the center of the primary, at the position of m3 in Fig. 2. (Note that this figure is not drawn to scale). The Cassegrain focus is located roughly 1 m past this elevation axis. In the Nasmyth configuration shown in Fig. 2, this focus is inside the hollow elevation bearing. The ellipsoidal mirror that is part of the relay optics (m5 in Fig. 2) will be moved to the new location along with SHARC-II.

Our polarimetry module will be installed near the Nasmyth focus. Before describing the optical design of the module that we intend to build, we will discuss a simpler design that illustrates the basic idea. This is shown in Figure 3. Light from the astrophysical source is reflected by the primary, the secondary, and the m3 flat of Fig. 2, and then enters Fig. 3 from the left. It passes through a half-wave plate and is then incident upon a pair of "crossed grids" that divide the beam into two orthogonal linearly polarized components which proceed along two different paths. (Crossed grids are commercially available from QMCI, Cardiff, Wales.) The polarization component that has E-vector parallel to the plane of the figure is reflected by mirrors B and C, and the other component (with E-vector perpendicular to the plane of the paper) proceeds along the path shown near the bottom of the figure. They approach one another again at D, which we refer to as the "combiner". The two polarization components are then imaged onto different ends of the "long-and-skinny" 12 x 32 SHARC-II array shown at the right of the figure. (In fact, they first must pass through the CSO relay optics m4 and m5, as shown in Fig. 2, but these are not shown in Fig. 3.)

With this polarimetry module installed, SHARC-II would function as a dual-beam polarimeter, observing both R and T polarization components (see section 1.3). This can be seen in Figure 3: The "top half" of the SHARC-II array will see the component of polarization that is parallel to the plane of the page while the "bottom half" of the array will see the component of polarization that is perpendicular to the plane of the page. However, these two "sub-arrays" will observe the same part of the sky, as can be seen by tracing the beams back from SHARC-II to the crossed grids at A. (We expect that each sub-array will consist of 12 x 12 pixels because it is likely that the central 8 x 12 pixel region will be unusable because of diffraction, misalignment, and other problems.) Note that a cold load must be used to terminate the unused polarization components (see Figure 3). To understand this, consider the beams that propagate from the pixels on the upper half of the SHARC-II array towards the combiner D. One component of polarization gets reflected upwards by the upper grid of the combiner, but the other passes through the grid. To avoid excess noise, this component must be terminated to a cold load.

As we have discussed, this very simple design cannot be realized at the CSO. The actual design that we will use is discussed below.

2. OPTICAL DESIGN

2.1 Simple polarimetry module

Figure 4 shows the simple optical design of Figure 3, but with actual rays drawn in. By placing the combiner at the Nasmyth focus we avoid wasting too many pixels near the center of the SHARC-II array which would otherwise "see" both orthogonal polarization components simultaneously and thus be useless. However, this figure shows why this simple version of our idea will fail: the Nasmyth focus is located at a point along the elevation axis that is within the elevation bearing tube (Fig. 2). This tube has an inner diameter much smaller that would be required to install a simple polarization module such as the one shown in Figures 3 and 4. Furthermore, another disadvantage of this simple design is that it introduces extra path length, that would have to be made up by moving SHARC-II and its relay optics forward, closer to the telescope. This would make it difficult to switch between photometric and polarimetric modes of operation.

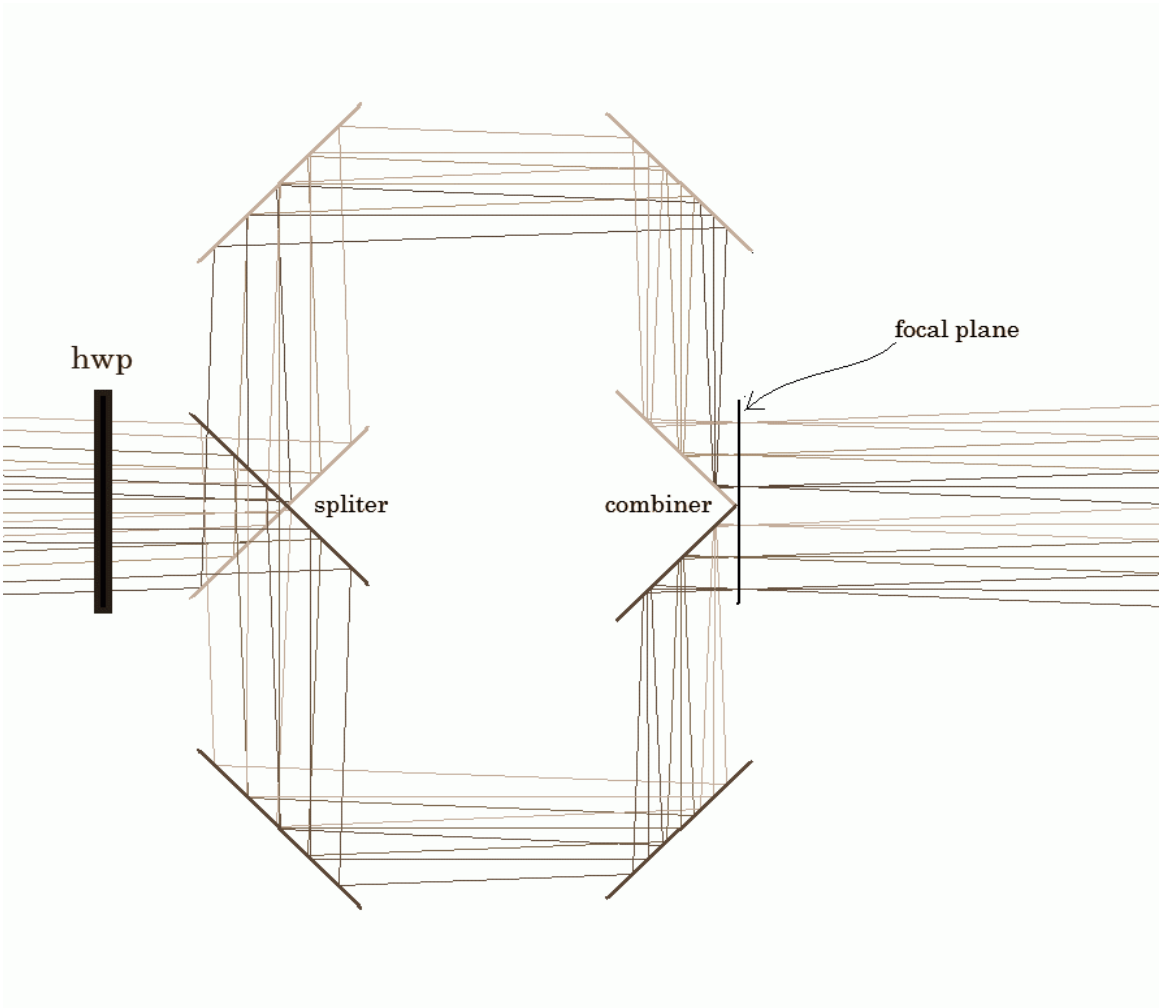

Fig. 4 - Another view of the simplifed version of the polarimetry module that we showed in Figure 3. Here we show the rays for six pixels of the SHARC-II array. The Nasmyth focus is at the position of the combiner.

Another problem with the simple polarimetry module of Figures 3 and 4 is related to primary mirror illumination. To understand this, follow the ray bundles shown in Figure 4, starting from any of the three pixels in the upper half of the array. Note that the central rays of these three bundles appear to be parallel as the bundles travel from the combiner upwards toward the mirror. In fact they are not parallel. They are defined by the pupil stop in SHARC-II, and thus they converge by just the right amount to ensure that when SHARC-II is used as a photometer (no polarimetry module) then each of its 12 x 32 pixels will illuminate the exact same region of the primary. In fact, there is also an image of the primary located very near to the location of the secondary, so all the pixels' beams will also overlap at this image

location. The convergence of the central rays is very slight, because the distance from the Nasmyth focus to the secondary is large.

If we could install our polarimetry module at the Nasmyth focus as shown in Figures 3 and 4 we would cause the two 12x12 sub-arrays to illuminate different portions of the primary. (They will also illuminate different portions of the image of the primary that is located near to the secondary.) We refer to this problem as differential primary illumination. It can be understood by noting that the effect of the polarimetry module on the outwards propagating beams from the pixels is to translate them laterally. Thus, the magnitude of the differential illumination, at the secondary, will be equal to the magnitude of the relative translation of the two orthogonal polarizations. The relative translation is about 5 cm and the secondary diameter is 60 cm, so the effect is not negligible. The improved design that we discuss in section 2.2 fixes all the problems of the simple design, except for the problem of differential primary illumination. This problem is reduced in amplitude, but is not eliminated.

2.2 Polarimetry module with re-imaging

Because the Nasmyth focus is inaccessible, we cannot use the simple design shown in Fig. 3 and Fig. 4. The simplest solution would be to re-image the Nasmyth focus to a more accessible location, and then install at this new location a polarimetry module similar to that of Fig. 3 and Fig. 4. This is what we plan to do, except that the re-imaging function and the polarimetry module function will be merged into a single optical design, as shown in Figure 5.

The re-imaging is accomplished with a pair of paraboloidal mirrors. The first converts each point in the Nasmyth focal plane into a collimated beam, and the second images this collimated beam to a new focus. These two paraboloidal mirrors are matched, so the f/# and magnification of the re-imaged focal plane are unchanged. Thus, no changes to the SHARC-II relay optics (nor to SHARC-II) are needed. Also, because of the manner in which we have folded the optical path, the installation of the module results in a virtual image at the location of the original Nasmyth image. As a result, SHARC-II and its relay optics will not have to be moved when switching between polarimetric and photometric modes of operation. It will be possible to change from polarimeter to photometer by removing just three small optical elements from the beam (see caption to Figure 5) rather than having to remove the entire polarimetry module.

Using the ZEMAX ray-tracing software, we have studied the optical performance of the design shown in Figure 5. We have done simulations spanning the range of pixel locations, chopping secondary tilt angles, and telescope elevation angles. (The latter is important to check when operating at Nasmyth.) We find that our polarimetry module does not introduce significant aberrations or distortion. However, there is one significant disadvantage to our design, which is differential primary illumination. The problem is different from what we described for the simple design (section 2.1). For the re-imaging design of Figure 5, any two pixels that view the same position on the sky in different polarizations will also be identical in terms of their primary mirror illumination. However, only the pixels that are near to the center of each sub-array will illuminate the primary properly. As one moves out to the edge pixels, the illumination becomes offset from the ideal, as shown in Figure 6. This is a consequence of the re-imaging. As far as we have been able to determine, it cannot be fixed without adding more reflections to an already complex system, so we have decided to live with this problem. We estimate that it will degrade the throughput by about 10% for edge pixels, with no degradation near the center of each sub-array.

For Hertz, the half-wave plate and grids are cold (4 K), but the SHARC-II polarimetry module will not be cooled. We expect 5-10% loss in the half-wave plate[19] which will degrade our signal-to-noise by 5-10%. Finally, we note that there are plans to install a K-mirror in front of SHARC-II, as a future upgrade after the intial move to the Nasmyth focus. This will likely necessitate a reconfiguration of our module, and a rethinking of the strategy for rapid changes between photometric and polarimetric modes of operation. However, we expect that the same optical components will be used and the same basic concepts will be employed.

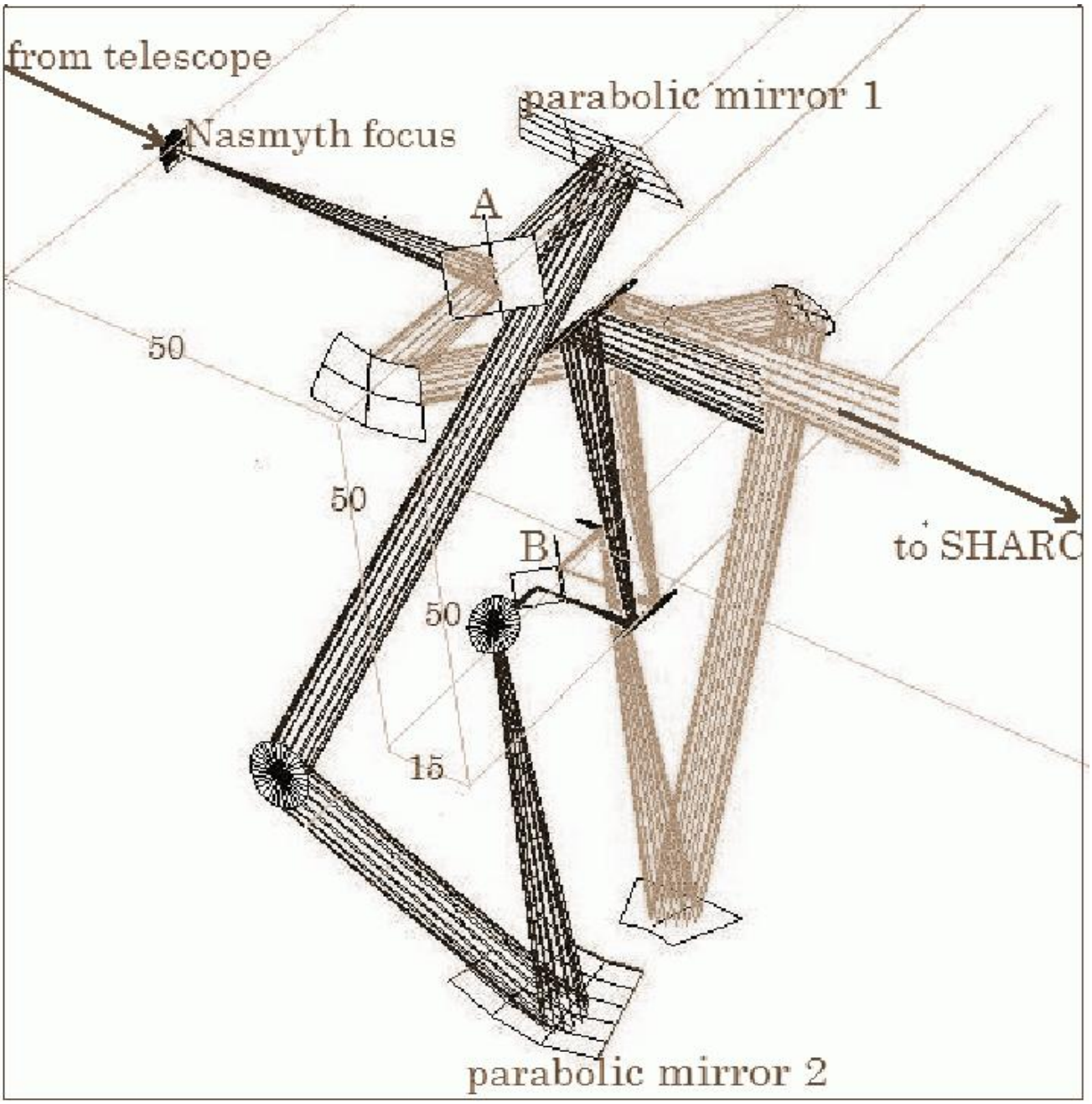

Fig. 5 - Simulation of optical design that we are implementing for our polarimetry module. Unlike the simple design shown in Fig. 3 and Fig. 4, this design incorporates re-imaging. The crossed grids are at A, and the combiner is at B. Between the crossed grids and the combiner, each polarization component passes through an optical path that includes two paraboloidal mirrors and two flat mirrors. The half-wave plate is not shown, but it will be between A and the Nasmyth focus. The cold load is also not shown, but it will be fed by another set of re-imaging optics. Dimensions are given in cm. SHARC-II can be converted back to photometry mode by removing the crossed grids, one flat mirror, and the half-wave plate mechanism. This simulation was done using the ZEMAX ray tracing software package.

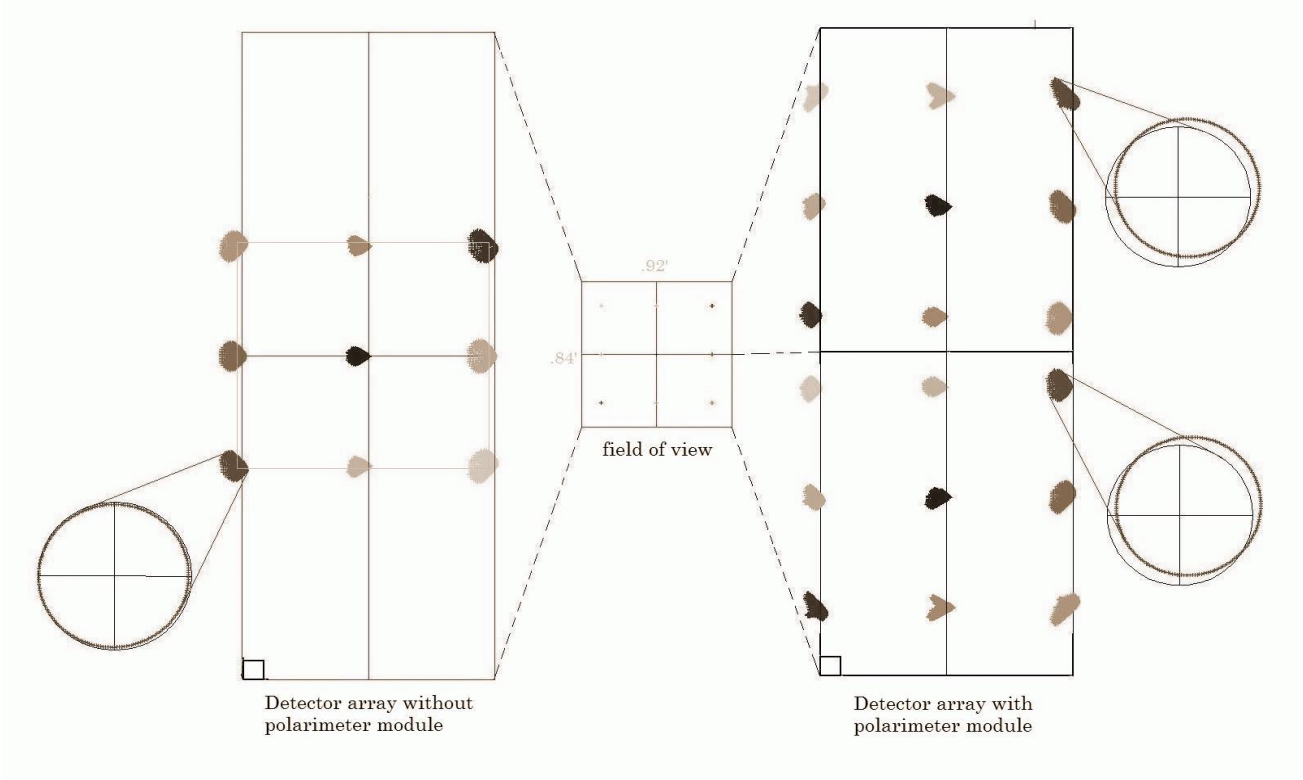

Fig. 6 - A comparison between images of point sources, for SHARC-II without the polarimetry module (left), and SHARC-II with the polarimetry module (right). The module used for this simulation is the one shown in Figure 5. Note that the module does not introduce any aberrations beyond those already present in the system, which are not very significant in comparison to the diffraction limit. For several pixels, the primary illumination is shown by comparing the image of the primary (dark circles) with the illumination of the primary (light circles). Note that the illumination is incorrect for the edge pixels with the polarimetry module installed. This problem is worst near the edges of each sub-array, and is absent near the center of each sub-array. ZEMAX was used for these simulations. The relative translation between the two polarization components corresponds to 15 pixels, but for the final design we expect this to be closer to 20 pixels so as to better utilize the array.

3. DATA ACQUISITION AND ANALYSIS

The basic data acquisition mode will be the same one used by our group in the past.[12,15] Specifically, we will make short photometric integrations at each of a series of half-wave plate positions, where each such integration involves fast chopping of the secondary and slower nodding of the telescope (see section 1.3). Note that the SHARC-II data acquisition system does support the chopping/nodding mode of photometric mapping, even though this is not the preferred method. (SHARC-II mapping is usually done by scanning the telescope in specific patterns without moving the secondary mirror.) Our polarimetry module's half-wave plate will be controlled by a dedicated computer that will interface to the SHARC-II data acquisition computer via tcp/ip socket.

Even though the basic data acquisiton mode is the same as what we have used in the past, the detailed observing strategy and the reduction algorithms will have to be different. The most important difference lies in the fact we will not follow the rotation of the sky. That is to say, the angular position of the array on the sky will depend on the parallactic, and elevation angles. These dependences are a result of the location of the instrument on the telescope, and how it will be used at the CSO.

Unlike Hertz, the SHARC-II polarimeter will (i) not be located at the CSO Cassegrain focus, but at a Nasmyth focus, and will (ii) not be positioned on a rotator to allow tracking the position angle of a given source as it moves across the sky. Point (i) also implies that the instrument will not be moving with the telescope in elevation, thus the dependence of the angular position of the array on the elevation angle. There will, therefore, be in each set of measurements three independent polarization components (from the source, the telescope, and the instrument) that will describe different trajectories in the (q,u)-plane (for the normalized Q and U Stokes parameters of linear polarization), as defined in the polarimeter's reference frame. The instrumental polarization will be fixed in the plane, while the telescope and source components will rotate in a predictable way as a function of the elevation and parallactic angles.

Our inability to track a source on the sky, or the telescope, with the SHARC-II polarimeter will force us to use different observing strategies than those used in the past. For example, it will not be possible to use the "Fixed Instrument", "Sky Tracking" or "Fast Rotation" techniques that our group has used in the past.[20] We will, however, still benefit from the dual-polarization detection capabilities of the polarimeter.

Also, we will incorporate into our data reduction scheme the noise removal techniques developed recently by L. Kirby and by H. Li[21]. In these schemes, the ratio $P = (R - T) / (R + T)$ is not formed immediately as the first step in the data analysis (see section 1.3 for definitions of variables). Rather, the quantities $D = R - T$, and $I = R + T$ are calculated separately, and the division is performed only after a sufficiently large amount of data is accumulated to ensure that I is accurately measured.

The result of the steps described above will be that for every pixel of each polarimetric observation, we will have Stokes parametrized signals that will be composed of a linear combination of polarized levels (of similar types) from the source (at different positions), the telescope, and the instrument. A polarization map of the source will be obtained by inverting the problem, after the data from each observation have been combined.

4. PREDICTED SPECIFICATIONS

Our sensitivity estimate, based on experience with the SHARC-II photometer and the Hertz polarimeter, is as follows: For a point source having a flux of 5 Jy at 350 microns, we will achieve 1% errors in 1 hour during the best 25% of winter nights. We also expect to be able to operate efficiently at 450 microns. The maximum chopper throw will be 8 arcminutes, just as for Hertz. As noted above, the angular resolution will be 9 arcseconds at 350 microns. We expect that queue scheduling will eventually be implemented for SHARC-II polarimetry observations.

This work has been supported by the National Science Foundation, via Award AST-0243156. It is a pleasure to acknowledge useful discussions with C. Borys, R. Chamberlin, A. Harper, and T. Phillips.

REFERENCES

1. R. H. Hildebrand, M. Dragovan, and G. Novak, "Detection of Submillimeter Polarization in the Orion Nebula", Ap. J. **284,** p. L51-L54, 1984.
2. J. S. Greaves et al., "A Submillimeter Imaging Polarimeter at the James Clerk Maxwell Telescope", MNRAS **340**, p. 353-361, 2003.
3. J. S. Greaves, in "Astronomical Polarimetry – Current Status and Future Directions", ASP Conference Series, in preparation.
4. B. C. Matthews, in "Astronomical Polarimetry – Current Status and Future Directions", ASP Conference Series, in preparation.
5. R. M. Crutcher, "Magnetic Fields in Molecular Clouds: Observations Confront Theory", Ap. J. **520**, p. 706-713, 1999.
6. A. Lazarian, in "Cosmic Evolution and Galaxy Formation: Structure, Interactions, and Feedback", ed. J. Franco, L. Terlevich, O. López-Cruz, & I. Aretxaga, ASP Conf. Ser. 215, p. 69, 2000.
7. D. K. Aitken, C. H. Smith, T. J. T. Moore, and P. F. Roche, "Mid-infrared Polarization Studies of SgrA: a Three-dimensional Study of the Central Parsec", MNRAS **299**, p. 743-752, 1998.
8. J. L. Dotson, J. A. Davidson, C. D. Dowell, D. A. Schleuning, and R. H. Hildebrand, "Far-Infrared Polarimetry of Galactic Clouds from the Kuiper Airborne Observatory", Ap. J. Supp. Ser. **128**, p. 335-370, 2000.
9. R. L. Akeson, J. E. Carlstrom, J. A. Phillips, and D. P. Woody, "Millimeter Interferometric Polarization Imaging of the Young Stellar Object NGC 1333/IRAS 4A", Ap. J. **456**, L45-L48, 1996.
10. J. M. Girart, R. M. Crutcher, and R. Rao, "Detection of Polarized CO Emission from the Molecular Outflow in NGC 1333 IRAS 4A", Ap. J. **525**, p. L109-L112, 1999.
11. D. K. Aitken, J. Greaves, A. Chrysostomou, T. Jenness, W. Holland, J. H. Hough, D. Pierce-Price, and J. Richer, "Detection of Polarized Millimeter and Submillimeter Emission from Sagittarius A*", Ap. J. **534**, p. L173-L176, 2000.
12. C. D. Dowell, R. H. Hildebrand, D. A. Schleuning, J. E. Vaillancourt, J. L. Dotson, G. Novak, T. Renbarger, and M. Houde, "Submillimeter Array Polarimetry with Hertz", Ap. J. **504**, p. 588-598, 1998.
13. M. Houde, C. D. Dowell, R. H. Hildebrand, J. L. Dotson, J. E. Vaillancourt, T. G. Phillips, R. Peng, and P. Bastien, "Tracing the Magnetic Field in Orion A", Ap. J. **604**, p. 717-740, 2004.
14. D. A. Schleuning, C. D. Dowell, R. H. Hildebrand, S. R. Platt, and G. Novak, "Hertz, A Submillimeter Polarimeter", PASP **109**, p. 307-318, 1997.
15. R. H. Hildebrand, J. A. Davidson, J. L. Dotson, C. D. Dowell, G. Novak, and J. E. Vaillancourt, "A Primer on Far-infrared Polarimetry", PASP **112**, p. 1215-1235, 2000.
16. C. D. Dowell et al., "SHARC II: a Caltech Submillimeter Observatory Facility Camera with 384 pixels", in "Millimeter and Submillimeter Detectors for Astronomy", eds. T. G. Phillips and J. Zmuidzinas, Proc. SPIE **4855**, p. 73-87, 2003.
17. T. Renbarger et al., "Early Results from SPARO: Instrument Characterization and Polarimetry of NGC 6334", PASP **116**, 415-424, 2004.
18. G. Novak et al., "First Results from the Submillimeter Polarimeter for Antarctic Remote Observations: Evidence of Large-scale Toroidal Magnetic Fields in the Galactic Center", Ap. J. **583**, L83-L86, 2003.
19. A. G. Murray, A. M. Flett, G. Murray, and P. A. R. Ade, "High Efficiency Half-wave Plates for Submillimetre Polarimetry", Infrared Physics **33**, p. 113-125, 1992.
20. S. R. Platt, R. H. Hildebrand, R. J. Pernic, J. A. Davidson, and G. Novak, "100 Micron Array Polarimetry from the Kuiper Airborne Observatory: Instrumentation, Techniques, and First Results", PASP **103**, p. 1193-1210, 1991.
21. H. Li, in "Astronomical Polarimetry – Current Status and Future Directions", ASP Conference Series, in preparation.